

Optimal Dose-Limited Phase Estimation without Entanglement

Stewart A. Koppell* and Mark A. Kasevich

Physics Department, Stanford University

(Dated: March 22, 2022)

Phase estimation is one of the most important facets of quantum metrology, with applications in sensing, microscopy, and quantum computation. When estimating a phase shift in a lossy medium, there is an upper bound on the attainable information per particle sent through the phase shift. Previously, only entanglement-enhanced measurements have been shown to saturate this bound. We introduce a measurement scheme which can saturate the bound without relying on entanglement.

I. INTRODUCTION

A central theme of quantum metrology is that entanglement in the probe state can enhance measurement precision. The NOON state interferometer, for example, achieves Heisenberg-limited precision using a maximally entangled n -particle probe[1]. While Heisenberg-limited measurements are often thought of as a uniquely quantum phenomenon, the same precision scaling is possible using a classical probe passed m times through the interferometer. In some treatments, n and m are defined as equivalent resources and multi-pass measurements are said to be Heisenberg-limited[2–4]. To clarify when a quantum advantage exists, it is important to carefully define the physical measurement resources and limitations.

When measuring a dynamical quantity such as in magnetometry or gravitational field detection, measurement bandwidth limits the maximum time the probe can coherently accrue its phase shift. Once this limit is saturated, the only way to increase sensitivity is with entanglement in the probe. In these applications, m and n may be optimized independently and the Heisenberg limit is exclusive to quantum measurements.

Phase estimation is also used in quantum computing as a subroutine for many important algorithms (e.g. Shor’s algorithm). Kitaev’s phase estimation algorithm [5] and the iterative phase estimation algorithm (IPEA) [6, 7] can achieve a precision scaling like $1/2^{nm}$ using n ancillary qubits and $m \log nm$ iterations [7]. Thus spatial resources (qubits) can be traded for temporal resources (runtime) while maintaining an exponential advantage.

The discrimination of unitary operations is another noteworthy measurement task where entanglement and multi-passing can be compared. In general, any single-pass measurement with a separable probe state repeated a finite number of times has a non-zero probability of failure. Perfect discrimination was first described as an application of entanglement [8, 9]. Later, in a letter which posed the question “What kind of tasks can be achieved without entanglement?”, it was shown that a multi-pass (MP) measurement can also suffice [10].

The primary interests of this Letter are applications like microscopy where the measurement is performed on a material sample which may be destroyed or altered by inelastic interactions with the probe. Assuming the sample can be modeled as a static phase shift, the goal is to maximize the information per dose d (probe intensity incident on the sample). For single-pass interferometer measurements, the dose metric simply counts the number of particles which enter the sample channel. A similar resource accounting is performed when the measurement has access to a strong local oscillator (i.e. none of the probe intensity needs to be allocated to a reference channel). For MP measurements, the dose metric takes into account the losses on each pass, which will reduce the dose inflicted on subsequent passes (in general, $d < n \times m$).

In optical microscopy, both entanglement-enhanced measurements[11–13] and MP measurements[14] have been shown to increase imaging sensitivity per dose. Similar schemes for improving the dose-limited resolution of transmission electron microscopes have been proposed[15–17]. However until now it has been unclear whether entanglement is necessary to achieve the best possible measurement sensitivity per dose.

We will employ the Quantum Fisher Information (QFI) formalism to address this question. Via the Quantum Cramer Rao Bound (QCRB), the QFI provides a lower limit on the error Δ_θ in an estimate of an unknown parameter θ [18–20]. If a measurement attaining QFI \mathcal{J} is repeated N times, the QCRB is

$$\Delta_\theta^2 \geq \frac{1}{N\mathcal{J}}. \quad (1)$$

The QFI for a lossless NOON-state interferometer is proportional to n^2 . This quadratic scaling, characteristic of the Heisenberg limit, is not the only hallmark of quantum advantage. In fact, in the presence of any amount of loss, the QFI cannot asymptotically scale better than n (the standard quantum limit)[21, 22]. Instead, quantum measurements may confer a constant advantage over the classical alternatives.

Using dose as a measurement resource, the figure of merit to optimize is $\xi = \mathcal{J}/d$, which we will refer to as the dose efficiency. For a sample with transmissivity η ,

* skoppell@mit.edu

the quantum limit is [21]

$$\xi_{\text{QL}} = \frac{4\eta}{(1-\eta)} . \quad (2)$$

Here we will describe a measurement which can saturate this limit without an entanglement-enhanced probe.

II. DOSE AS A MEASUREMENT RESOURCE

It will be instructive to begin by calculating ξ for several well-known measurements. A standard approach to calculating the QFI in the presence of loss involves Kraus operators, which describe the dynamics of open quantum systems[23–25]. We can take simpler approach when the probe is a pure single-particle state or a NOON state.

As a result of possible absorption, the exit state will generally be mixed: $\rho = \sum p_i |\psi_i\rangle\langle\psi_i|$. If $\mathcal{J}[\psi_i]$ is the QFI for ψ_i , then $\mathcal{J}[\rho] \leq \sum p_i \mathcal{J}[\psi_i]$ (i.e. the QFI is convex). The equality holds only when each $|\psi_i\rangle$ is measured optimally in the same basis. When the absorption of a single particle projects the probe into a state which yields no information, then $\mathcal{J} = p\tilde{\mathcal{J}}$ where $\tilde{\mathcal{J}}$ is the QFI conditional on no absorption, which happens with probability p .

We begin with a lossy Mach-Zehnder interferometer (MZI) using a single-particle probe. If α is the amplitude sent to the sample arm, the normalized exit wavefunction is

$$\psi(\theta) = \frac{1}{\sqrt{p}} \begin{bmatrix} \sqrt{1-\alpha^2} \\ \alpha\sqrt{\eta}e^{i\theta} \end{bmatrix} . \quad (3)$$

with $p = 1 - (1-\eta)\alpha^2$. The QFI for a pure state is [18]

$$\mathcal{J} = 4\langle\dot{\psi}|\dot{\psi}\rangle - 4|\langle\dot{\psi}|\psi\rangle|^2 , \quad (4)$$

where the dot indicates a derivative with respect to θ . So the the lossy MZI has

$$\tilde{\mathcal{J}} = \frac{4}{p}|\alpha|^2\eta \left(1 - \frac{1}{p}|\alpha|^2\eta\right) . \quad (5)$$

The expected QFI per dose $d = |\alpha|^2$ is maximized in the limit $\alpha \rightarrow 0$, yielding

$$\xi = \frac{p\tilde{\mathcal{J}}}{d} = 4\eta . \quad (6)$$

The principle that the dose efficiency is maximized when the intensity in the sample channel is infinitesimal will be true for each of the measurements we discuss below (when α is strictly zero, the measurements provide no information). Compared to the quantum limit, the MZI yields less information per dose by a factor of $1/(1-\eta)$, which diverges as $\eta \rightarrow 1$.

In the presence of loss, NOON state interferometers are sub-optimal because they fail when a single particle is absorbed. Nevertheless, an unbalanced NOON

state (with probability $|\alpha|^2 \ll 1$ of finding n particles in the sample channel and probability $1 - |\alpha|^2$ of finding n particles in the reference channel) is a significant improvement over a single particle probe for a MZI. For $\eta \sim 1$, $\xi_{\text{NOON}}/\xi_{\text{QL}} \gtrsim 1/e$ for optimal n . Explicitly, $\mathcal{J} = 4n^2\eta^n|\alpha|^2$ and $d = n|\alpha|^2$, so

$$\xi_{\text{NOON}} = 4n\eta^n . \quad (7)$$

which is maximized by choosing $n \sim -1/\ln \eta$.

MP and NOON state interferometers provide the same \mathcal{J} when $n = m$ and are both spoiled by a single absorption. However, the dose from a MP measurement is limited: there can be no more than a one absorption. As a result, MP measurements can be more dose efficient. For optimal m , $\xi_{\text{MP}}/\xi_{\text{QL}} \gtrsim 0.65$, and in general $J = 4m^2\eta^m$ and $d = \sum_{k=0}^{m-1} \eta^k$ so

$$\xi_{\text{MP}} = 4m^2\eta^m \frac{1-\eta}{(1-\eta^m)} . \quad (8)$$

While a MP interferometer does not fully achieve the quantum limit, the simplicity of the scheme may make it the practical choice in many applications.

The expected number of particles in a pure single mode Gaussian state is $\langle n \rangle = \alpha^2 + \sinh^2(r)$ where α is the displacement parameter and r is the squeezing parameter (measured in dB, the squeezing is $20 \ln r/10$). The number of particles contributing to the squeezing is $n_{\text{sq}} = \sinh^2(r)$. If $\langle n \rangle \gg n_{\text{sq}}$, then [26]

$$\xi_{\text{SQZ}}(n_{\text{sq}}) = \frac{4\eta}{2\eta n_{\text{sq}} - 2\eta\sqrt{(n_{\text{sq}}(n_{\text{sq}}+1))} + 1} . \quad (9)$$

When n_{sq} is large, the denominator approaches $1-\eta$ and this measurement saturates the quantum limit for dose efficiency.

Fig. 1 Shows ξ/ξ_{QL} for each of these measurements vs (A) the absorption probability $1-\eta$ and (B) the relevant measurement parameter (m , n , or n_{sq}) with $\eta = 0.9$.

III. PHASE ESTIMATION WITH A CHAIN INTERFEROMETER

The most general possible m -stage entanglement-free phase estimation scheme could use up to m auxiliary channels in addition to the sample channel, with unitary transformations applied to couple all the channels between each stage. This would likely be infeasible to implement as a microscope architecture. We will show that an optimal measurement is possible using only two channels in a configuration we call a chain interferometer (CI). Figure 2 shows a CI with m stages. At each stage, a beamsplitter couples the reference channel to a sample channel. In practice, the measurement may be applied to a single, unique sample by using fast-switching optics to fold the optical path onto itself, in which case only one beamsplitter is required. This architecture has been

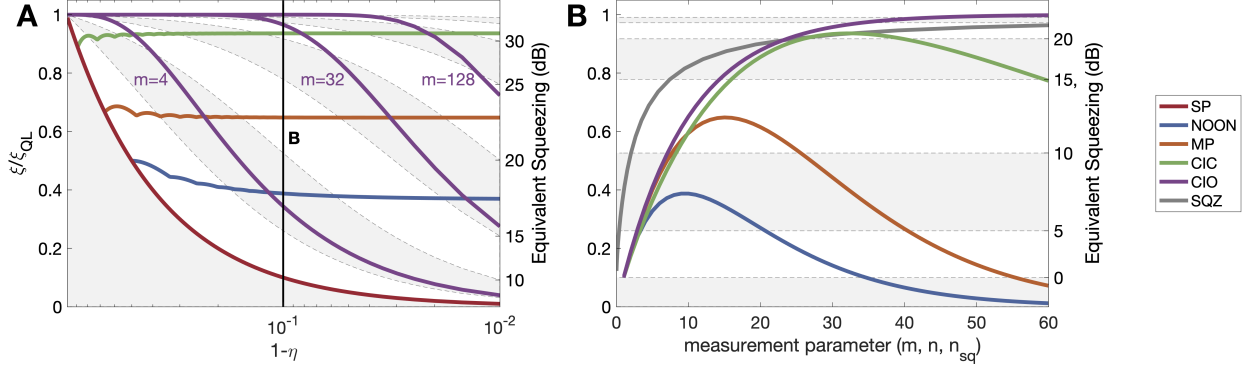


FIG. 1. QFI per dose (ξ) relative to the quantum limit (ξ_{QL}) for measurements with: a single particle probe and single-pass (SP), a maximally entangled probe of size n (NOON), a single-particle passed m times through the sample (MP), an m -stage chain interferometer with constant beamsplitter angles (CIC), an m -stage chain interferometer with optimized beamsplitter angles (CIO), and a squeezed Gaussian probe state (SQZ) with n_{sq} particles contributing to the squeezing. (A) ξ/ξ_{QL} vs probability of absorption by the sample (for each particle on each pass). For the NOON, MP, and CPC measurements, m and n are optimal. The CIO measurement performance is calculated for $m=4, 32$, and 128 stages. The striped background shows the amount of squeezing (in dB) needed for a Gaussian probe to have equivalent performance. (B) ξ/ξ_{QL} vs the relevant measurement parameter for $\eta = 0.9$ (marked by a vertical black line in (A)).

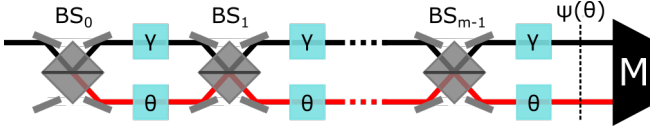


FIG. 2. Chain interferometer scheme for estimation of an unknown phase θ . In each of m stages, the reference channel (black) and sample channel (red) are weakly coupled with a beamsplitter (BS) before the probe interacts with the unknown phase shift in the sample arm and a programmed phase shift in the reference arm. The result is output wavefunction $\psi(\theta)$. The QFI of $\psi(\theta)$ is related to the variance in the estimate of θ using an optimal measurement M .

proposed before in the context of interaction-free measurement (IFM), where the presence of an absorber in the sample channel can be detected with an arbitrarily small chance of damage (loss)[27].

The CI can be optimized by adjusting m , the beamsplitter transmissivity T , and reference phase shift γ . When $\gamma = 0$ and $T = \sin(\pi/2m)^2$, the CI implements IFM. However this configuration does not saturate the quantum limit for dose-limited phase estimation. This architecture has been numerically optimized in Ref. [26], which found that when $T \approx (0.01/2m)^2$ and $\gamma = 0$ (assuming small θ), the CI could attain $\xi/\xi_{\text{QL}} > 0.9$.

We will take a more analytical approach and allow the beamsplitter transmissivity to change for each stage. We could also allow the reference phase shift to change for each stage, but this turns out to be unnecessary. Given the discussion in Section II, we will allocate the majority of the probe amplitude to the reference arm with the ansatz $T_k < \epsilon^2$ for some $\epsilon \ll 1$. We will also set $\gamma \sim \theta$ (this choice requires some prior knowledge of the

θ , which is always an implicit assumption of the QFI formalism[18]).

Unlike a simple MP interferometer, the exit wavefunction of a CI contains terms corresponding to different numbers of passes through the sample. Interference between these terms provides extra information. The details of calculating \mathcal{J} and d are given in the supplementary material. To order ϵ^2 ,

$$\mathcal{J} = 4 \left| \sum_{k=0}^{m-1} (m-k) \eta^{(m-k)/2} \tau_k \right|^2 \quad (10)$$

where $\tau_k = \sqrt{T_k}$ and

$$d = \sum_{k=0}^{m-1} \left| \sum_{k'=0}^k \eta^{(k-k')/2} \tau_{k'} \tau_k \right|^2. \quad (11)$$

We found the set of τ_k which maximize ξ by analytically solving the $m = 2$ and $m = 3$ case and extrapolating. The result is

$$\tau_k = \begin{cases} \epsilon \eta^{m/2} & k = 0 \\ \epsilon (1 - \eta) \eta^{(m-k)/2} & k > 0 \end{cases}.$$

Using this prescription, we find

$$\lim_{m \rightarrow \infty} \mathcal{J} = \epsilon^2 \frac{4\eta^2}{(1-\eta)^2} \quad \text{and} \quad \lim_{m \rightarrow \infty} d = \epsilon^2 \frac{\eta}{1-\eta}. \quad (12)$$

so that $\xi \rightarrow \xi_{\text{QL}}$ for large m .

In Fig. 1 (A) and (B), the lines labeled CIC are ξ/ξ_{QL} for a CI with a constant, infinitesimal beamsplitter transmissivity using the optimal number of stages. The lines labeled CIO show ξ/ξ_{QL} for a CI with optimized beamsplitter transmissivities. For $\eta = 0.9$, a 10(32)-stage CI

(using either strategy) is more dose efficient than a standard interferometer using a Gaussian probe squeezed by 10(20) dB.

IV. OPTICAL LOSSES

So far we have neglected losses other than those caused by the sample. We will now consider the effects of loss during probe preparation (probability $1 - \eta_P$), loss between each stage of a MP or chain interferometer (probability $1 - \eta_{rt}$), and loss during detection (probability $1 - \eta_D$).

Loss during probe preparation decreases intensity without affecting the dose efficiency for single-particle measurements. However this type of loss can still reduce the effectiveness of entangled probes. For squeezed states, this loss injects vacuum noise, putting a ceiling on the maximum effective squeezing. For the same reason, entanglement-enhanced measurements also suffer disproportionately from loss at the detection stage.

The dose efficiencies for each of the measurements discussed so far are derived in the supplemental document. For CI and squeezed-state measurements, the dose efficiency has upper bound

$$\xi \leq \frac{4\eta\eta_D}{(1 - \eta\eta^*)}, \quad (13)$$

which is saturated in the limit $m \rightarrow \infty$ or $n_{sq} \rightarrow \infty$, respectively. For a CI, $\eta^* = \eta_{rt}$, and for a squeezed state interferometer, $\eta^* = \eta_P\eta_D$. When $\eta_{rt} < \eta_P\eta_D$, the CI has superior performance. The optimal beamsplitter transmissivities τ_k are adjusted in the presence of loss as described in the supplementary material.

It may be possible to build a MP interferometer with lower loss than is possible with a CI. If, for example, $\eta_{rt} = 0.99$ for MP, then it becomes more effective than CIO with $\eta_{rt} = 0.95$ for $\eta > 0.94$. Low MP loss also makes it feasible to combine multi-passing and squeezing. A multi-pass squeezed state interferometer (with $\eta_{rt} = 0.99$) surpasses CIO (with $\eta_{rt} = 0.95$) for $\eta > 0.84$.

In Fig 3 we show the dose efficiency of measurements with $\eta_{rt} = 0.95$ and $\eta_P = \eta_D = 0.9$ relative to the quantum limit for $\eta_{rt} = \eta_P = \eta_D = 1$.

V. CONCLUSION

We have identified a new type of phase estimation protocol which attains the quantum limit for information per dose without using entanglement. This makes it possible, in principle, to employ a quantum-optimal measurement in microscopy using only basic optical elements. When taking into account losses in the optics for forming the probe and performing the measurement of the exit wavefunction, we found single-particle multi-stage measurements can potentially outperform the best known entanglement-enhanced measurements.

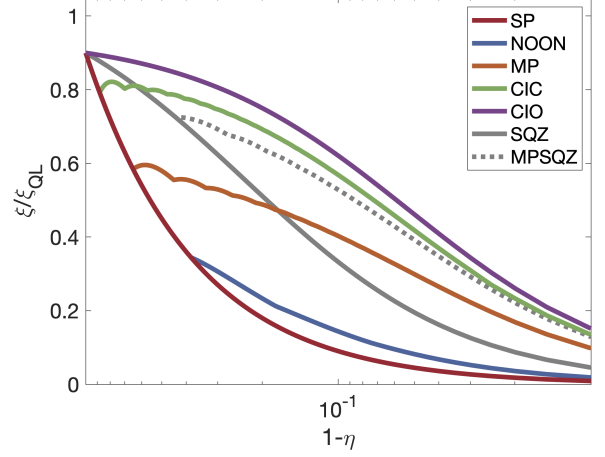


FIG. 3. QFI per dose with optical losses outside of the sample. We assume 10% loss during both probe preparation and detection and 5% loss at each stage of the MP and CI measurements. The measurements are as described in Fig. 1. The curve labeled SQZ represents the upper bound on squeezing enhancement ($n_{sq} \rightarrow \infty$), and the dotted line labeled MPSQZ is the bound measurements with both squeezing and multiple passes.

Appendix A: Dose efficiency for a CI

Let $\psi_j^{(k)}$ be the wavefunction just before encountering the sample on pass k (numbered $k = 0$ to $k = m - 1$), with index $j = 0$ and $j = 1$ referring to the reference and sample channels, respectively. We will assume the probe is a single particle in initial state

$$\psi^0 = \begin{bmatrix} 1 \\ 0 \end{bmatrix}. \quad (A1)$$

The output wavefunction will be written ψ_j . We will assume that the coupling between the reference and sample channels is infinitesimal. As a result, the QFI can be written

$$\mathcal{J} = 4p \langle \dot{\psi}_j | \dot{\psi}_j \rangle \quad (A2)$$

where $1 - p$ is the probability that the sample absorbs the probe. The dose is defined as

$$d = \sum_{k=0}^{m-1} \left| \dot{\psi}_1^{(k)} \right|^2. \quad (A3)$$

Let B_k and S be operators representing actions of the beamsplitters and sample, respectively:

$$B_k = \begin{bmatrix} \sqrt{1 - \tau_k^2} & \tau_k \\ \tau_k & \sqrt{1 - \tau_k^2} \end{bmatrix} \quad (A4)$$

and

$$S_k = \begin{bmatrix} 1 & 0 \\ 0 & \sqrt{\eta} e^{i\theta} \end{bmatrix}. \quad (A5)$$

With the assumption that the beamsplitter transmissivity is small ($\tau_k < \epsilon \ll 1$), we can ignore terms of order ϵ^3 and higher. To this order, the output wavefunction is

$$\begin{bmatrix} \psi_0 \\ \psi_1 \end{bmatrix} = \frac{1}{\sqrt{p}} \begin{bmatrix} 1 - \frac{1}{2} \sum_k \tau_k^2 - \sum_{k>k'} \tau_k \tau_{k'} \eta^{(k'-k)/2} e^{i(k-k')\theta} \\ - \sum_k \tau_k \eta^{(m-k)/2} e^{i(m-k)\theta} \end{bmatrix}. \quad (\text{A6})$$

Using equations A2 and A3, we arrive at the expressions for \mathcal{J} and d found in the main text. Notice that

$$|\langle \psi_j | \psi_j \rangle|^2 \sim \mathcal{O}(\epsilon^4),$$

justifying the approximation in A2.

Appendix B: Formulas for ξ with optical loss

If $1 - \eta_P$ and $1 - \eta_D$ are the losses during probe preparation and detection, respectively, then an MZI with intensity $|\alpha|^2 \ll 1$ in the sample arm has

$$\mathcal{J} = 4\eta_P \eta_D |\alpha|^2, \quad \text{and} \quad d = \eta_P |\alpha|^2$$

so

$$\xi = 4\eta \eta_D. \quad (\text{B1})$$

If the loss between passes in a MP interferometer is $1 - \eta_{\text{rt}}$, then

$$J = 4m^2 \eta_P \eta^m \eta_{\text{rt}}^{m-1} \eta_D \quad \text{and} \quad d = \eta_P \sum_{k=0}^{m-1} (\eta_{\text{rt}} \eta)^k,$$

so

$$\xi_{\text{MP}} = 4m^2 \eta^m \eta_{\text{rt}}^{m-1} \eta_D \frac{1 - \eta_{\text{rt}} \eta}{1 - (\eta_{\text{rt}} \eta)^m} \quad (\text{B2})$$

Notice ξ is independent of η_P for MP and SP measurements: loss during probe preparation prolongs the measurement but does not affect dose efficiency. This will also be the case for a CI, but not for measurements with an entangled probe.

For single-pass entanglement-enhanced measurements, the location of the absorption will not affect \mathcal{J} (though it may effect d). For a NOON state interferometer with n -particle amplitude α in the sample arm,

$$\mathcal{J} = 4n^2 (\eta_P \eta \eta_D)^n \quad \text{and} \quad d = \eta_P n |\alpha|^2$$

so

$$\xi_{\text{NOON}} = 4n \eta_P^{n-1} (\eta \eta_D)^n. \quad (\text{B3})$$

For a squeezed-state interferometer with total loss η_{tot} (with large n_{sq}),

$$\mathcal{J} = \frac{4|\alpha|^2 \eta_{\text{tot}}}{1 - \eta_{\text{tot}}}$$

Using $\eta_{\text{tot}} = \eta_P \eta \eta_D$ and $d = |\alpha|^2 \eta_P$,

$$\xi_{\text{SQZ}} = \frac{4\eta \eta_D}{1 - \eta_P \eta \eta_D} \quad (\text{B4})$$

When there is no loss outside of the sample, then single-pass squeezing is an optimal strategy. However, depending on the size of η_{rt} relative to η_P and η_D , a MP squeezed-state measurement can outperform squeezing or MP alone. The total loss is $\eta_{\text{tot}} = \eta_P \eta^m \eta_{\text{rt}}^{m-1} \eta_D$ and

$$\mathcal{J} = \frac{4|\alpha|^2 m^2 \eta_{\text{tot}}}{1 - \eta_{\text{tot}}}, \quad d = |\alpha|^2 \eta_P \frac{1 - (\eta_{\text{rt}} \eta)^m}{1 - \eta_{\text{rt}} \eta}.$$

Finally, a lossy CI with has

$$\mathcal{J} = 4\eta_P \eta_{\text{rt}}^{m-1} \eta_D \left| \sum_{k=0}^{m-1} (m-k) \eta^{(m-k)/2} \tau_k \right|^2, \quad d = \eta_P \sum_{k=0}^{m-1} \eta_{\text{rt}}^k \left| \sum_{k'=0}^k \eta^{(k-k')/2} \tau_{k'} \right|^2$$

and the set of τ_k which maximize ξ are:

$$\tau_0 = \epsilon (\eta_{\text{rt}} \sqrt{\eta})^m \quad \tau_{k>0} = \epsilon (1 - \eta_{\text{rt}} \eta) (\eta_{\text{rt}} \sqrt{\eta})^{m-k}$$

giving

$$\xi_{\text{CI}} = \frac{4\eta \eta_D}{1 - \eta \eta_{\text{rt}}} \quad (\text{B5})$$

in the limit of large m .

-
- [1] M. J. Holland and K. Burnett, Interferometric detection of optical phase shifts at the heisenberg limit, Phys. Rev. Lett. **71**, 1355 (1993).
[2] B. Higgins, D. W. Berry, S. D. Bartlett, H. M. Wiseman, and G. J. Pryde, Entanglement-free heisenberg-limited phase estimation, Nature **450**, 393 (2007).

- [3] M. de Burgh and S. D. Bartlett, Quantum methods for clock synchronization: Beating the standard quantum limit without entanglement, Phys. Rev. A **72**, 042301 (2005).
[4] A. Luis, Phase-shift amplification for precision measurements without nonclassical states, Phys. Rev. A **65**,

- 025802 (2002).
- [5] A. Y. Kitaev, Quantum measurements and the abelian stabilizer problem, *Electron. Colloquium Comput. Complex.* **3** (1996).
 - [6] R. B. Griffiths and C.-S. Niu, Semiclassical fourier transform for quantum computation, *Phys. Rev. Lett.* **76**, 3228 (1996).
 - [7] M. Dobříček, G. Johansson, V. Shumeiko, and G. Wendin, Arbitrary accuracy iterative quantum phase estimation algorithm using a single ancillary qubit: A two-qubit benchmark, *Phys. Rev. A* **76**, 030306 (2007).
 - [8] A. Acín, Statistical distinguishability between unitary operations, *Phys. Rev. Lett.* **87**, 177901 (2001).
 - [9] G. M. D'Ariano, P. Lo Presti, and M. G. A. Paris, Using entanglement improves the precision of quantum measurements, *Phys. Rev. Lett.* **87**, 270404 (2001).
 - [10] R. Duan, Y. Feng, and M. Ying, Entanglement is not necessary for perfect discrimination between unitary operations., *Physical review letters* **98** **10**, 100503 (2007).
 - [11] P. C. Humphreys, M. Barbieri, A. Datta, and I. A. Walmsley, Quantum enhanced multiple phase estimation, *Physical review letters* **111**, 070403 (2013).
 - [12] Y. Israel, S. Rosen, and Y. Silberberg, Supersensitive polarization microscopy using noon states of light, *Physical review letters* **112**, 103604 (2014).
 - [13] C. A. Casacio, L. Madsen, A. Terrasson, M. Waleed, K. Barnscheidt, B. Hage, M. Taylor, and W. Bowen, Quantum-enhanced nonlinear microscopy., *Nature* **594** **7862**, 201 (2021).
 - [14] T. Juffmann, B. B. Klopfer, T. L. Frankort, P. Haslinger, and M. A. Kasevich, Multi-pass microscopy, *Nature Communications* , 1 (2016).
 - [15] H. Okamoto and Y. Nagatani, Entanglement-assisted electron microscopy based on a flux qubit, *Applied Physics Letters* **104** (2013).
 - [16] W. P. Putnam and M. F. Yanik, Noninvasive electron microscopy with interaction-free quantum measurements, *Physical Review A* **80**, 040902 (2009).
 - [17] T. Juffmann, S. A. Koppell, B. B. Klopfer, C. Ophus, R. M. Glaeser, and M. A. Kasevich, Multi-pass transmission electron microscopy, *Scientific Reports* **7**, 1 (2017).
 - [18] A. S. Holevo, *Probabilistic and Statistical Aspects of Quantum Theory* (Amsterdam: North- Holland, 1982).
 - [19] C. W. Helstrom, Minimum mean-squared error of estimates in quantum statistics, *Physics Letters A* **25**, 101 (1967).
 - [20] S. L. Braunstein and C. M. Caves, Statistical distance and the geometry of quantum states, *Phys. Rev. Lett.* **72**, 3439 (1994).
 - [21] B. Escher, R. Filho, and L. Davidovich, General framework for estimating the ultimate precision limit in noisy quantum-enhanced metrology, *Nature Physics* **7** (2012).
 - [22] R. Demkowicz-Dobrzański, J. J. Kolodyński, and M. Guta, The elusive heisenberg limit in quantum-enhanced metrology, *Nature Communications* **3**, 1063 (2012).
 - [23] U. Dorner, R. Demkowicz-Dobrzański, B. J. Smith, J. S. Lundeen, W. Wasilewski, K. Banaszek, and I. A. Walmsley, Optimal quantum phase estimation, *Phys. Rev. Lett.* **102**, 040403 (2009).
 - [24] R. Demkowicz-Dobrzański, U. Dorner, B. J. Smith, J. S. Lundeen, W. Wasilewski, K. Banaszek, and I. A. Walmsley, Quantum phase estimation with lossy interferometers, *Phys. Rev. A* **80**, 013825 (2009).
 - [25] R. Demkowicz-Dobrzański, M. Jarzyna, and J. Kołodyński, Chapter four - quantum limits in optical interferometry (Elsevier, 2015) pp. 345–435.
 - [26] P. M. Birchall, J. L. O'Brien, J. C. F. Matthews, and H. Cable, Quantum-classical boundary for precision optical phase estimation, *Phys. Rev. A* **96**, 062109 (2017).
 - [27] P. Kwiat, H. Weinfurter, T. Herzog, A. Zeilinger, and M. A. Kasevich, Interaction-free measurement, *Physical Review Letters* **74**, 4763 (1995).